Neutron Diffraction Studies of Novel Complex Hydrides

YANG Jinbo[1], Yelon W B[2], James W J[2]

(1. State Key Laboratory for Mesoscopic Physics, Department of Phsics, Peking University, Beijing 100871, China)
(2. Materials Research Center, Missouri University of Science and Technology, Rolla, MO 65409, USA)

Abstract: The crystal structures of Li_2NH, $LiNH_2$, $Li_4BN_3H_{10}$, and BH_3NH_3 have been investigated using powder neutron diffraction with high sensitivity. The lattice parameters and the atomic positions were determined using Rietveld refinement. These studies have revealed differences between studies conducted with x-rays and by neutrons, using deuterated compounds, and have shown some systematic trends between bond lengths and decomposition temperatures. The mixture of different hydrides such as $LiBH_4$ and $LiNH_2$ may provide new materials to meet hydrogen storage targets through changing the hydrogen host bond, such as N-H, B-H bonds.

Key words: hydrogen storage materials; neutron diffraction; crystal structure

新型储氢材料的中子衍射研究

杨金波[1], Yelon W B[2], James W J[2]

(1. 北京大学物理学院，人工微结构和介观物理国家重点实验室，北京 100871)
(2. 美国密苏里科技大学材料研究中心，罗拉市 密苏里州 65409)

摘　要: 利用高灵敏度中子粉末衍射对新型储氢材料 Li_2NH, $LiNH_2$, $Li_4BN_3H_{10}$ 和 BH_3NH_3 的晶体结构进行了研究。通过对中子衍射数据的拟合分析得到了材料的晶格参数，原子占位和键长等数据。研究发现测量的氢原子占位结果与 X − 光衍射测量的结果有明显差别。结果表明储氢材料的氢释放温度与材料中的 N-H 或 B-H 键的键长成对应关系。通过将不同的储氢材料，例如 $LiBH_4$ 和 $LiNH_2$，进行复合改变材料中 N-H 和 B-H 氢键的强度，可以合成新的材料，有望达到储氢的目标。

关键词: 储氢材料；中子衍射；晶体结构

1　Introduction

The requirements for hydrogen storage have been spelled out in numerous DOE reports, and include both volumetric and gravimetric reversible hydrogen density requirements, that include the mass of the fuel delivery system(storage and reactor, if necessary). None of the currently favored systems meet these requirements, but many of them serve as models for fundamental studies of the relationship of hydrogen bonding to decomposition kinetics. One complex hydride, $NaAlH_4$ (catalyzed by $TiCl_3$) has favorable kinetics and reversibility, but fails, by a significant factor to meet the density requirements[1−5]. Other systems, such as $LiBH_4$ meet

the density requirements, but do not decompose at low enough temperatures and are not reversible[5−8]. Chemical hydrides such as NH_3BH_3[9−11], have better kinetics and capacity, but appear not to be reversible due to the formation of polymeric chains during the decomposition. The total capacity of that system cannot be utilized since the final product, BN, is too stable to allow reversibility. Nevertheless, studies of these materials provide vital information about the detailed structures, the bond lengths and other parameters, which can serve as data for calculations, used to better understand the thermodynamics of the systems, and for modeling of novel materials that might provide the optimum combination of thermodynamic properties and capacity[12−16]. Since neutron diffraction is the best tool for the accurate determination of the position of hydrogen/deuterium in crystal structures, it is an essential component in any program to fully understand and develop hydrogen storage systems based on hydrides. In the present paper, we have used neutron

powder diffraction to determine the crystal structures for LiNH$_2$, Li$_2$NH and Li$_4$BN$_3$H$_{10}$ and BH$_3$NH$_3$.

2 Methods

The powder neutron diffraction (ND) experiments were performed on the position sensitive detector diffractometer at the University of Missouri Research Reactor using neutrons of wavelength $\lambda = 0.148\ 75$ nm. The data for as-prepared and annealed samples were collected over 24 h at different temperatures between 2θ angles of 5 and 105 degree on approximately 1.0 g of fine powders. The refinement of the neutron diffraction data was carried out using the FULLPROF program which permits multiple phase refinement.

3 Results and Discussion

3.1 Li$_2$NH

Recently, the Li-N-H system(Li$_3$N, LiNH$_2$ and LiH) has attracted much attention as a promising novel hydrogen storage material. Chen et al[17], have demonstrated the reversible absorption/desorption of hydrogen via the formation of lithium imide(Li$_2$NH): LiNH$_2$ + LiH $\Longleftrightarrow$ Li$_2$NH + H$_2$. The performance of Li$_2$NH as a hydrogen storage material is strongly dependent on the preparative methods. It was reported that Li$_2$NH prepared via reaction between Li$_3$N and Li$_2$NH shows much higher reversible hydrogen storage capacity with fast kinetics and excellent stability as compared to those prepared via the conventional LiNH$_2$ decomposition method[18]. However, the mechanism of the hydrogenation/ dehydrogenation in the Li-N-H system is still not clear, in large part owing to the lack of accurate crystal structures of LiNH$_2$ and Li$_2$NH.

We have prepared Li$_2$NH compounds using different synthesis pathways: (1)2LiNH$_2$ = Li$_2$NH + NH$_3$, (2)Li$_3$N + LiNH$_2$ = 2Li$_2$NH, (3)LiH + LiNH$_2$ = Li$_2$NH + H$_2$. Neutron diffraction at different temperatures has been used to study the crystal structure and possible phase transitions of Li$_2$NH. It was found that the crystal structure and phase transition are related to the synthesis methods. A phase transition from the low temperature phase 16 K ~ 350 K to the high temperature phase above 370 K has been confirmed for the sample prepared by reacting Li$_3$N with LiNH$_2$ (see Fig. 1a). The low temperature phase (α-Li$_2$NH) could be described as disordered cubic(Fd-3m) structure with a lattice parameter a about 1.02 nm. Li atoms occupy 48f, 8a, and partially 32e sites. N and H atoms fully occupy 32e sites, respectively. The high temperature phase was also indexed as cubic(Fm-3m) structure with a lattice parameter a about 0.512 nm. The Li$_2$NH (β-Li$_2$NH) prepared by decomposition of LiNH$_2$ shows only the high temperature phase (Fig. 1b). The reaction of LiH + LiNH$_2$ at 300 ℃ for 24 h under vacuum produces some Li$_2$NH(γ-Li$_2$NH) with partially unreacted LiNH$_2$ and LiH as impurities(Fig. 1c). There is no phase transition in the temperature range from 16 K to 400 K for β- and γ-Li$_2$NH phases. α-Li$_2$NH exhibits a higher reversible hydrogen storage capacity and faster kinetics. The structural differences among the lithium imides may lead to different reaction mechanisms for hydrogen absorption/desorption in the Li-N-H system.

β-and γ-Li$_2$NH have a cubic structure at room temperature with partial disorder of the H atoms. Several different space groups can be used to describe the structure, and detailed analysis is required to determine the most probable structure and the associated N-H bond length. The neutron diffraction data(Figs. 1b and c) were modeled in Fd-3m, F-43m and Fm-3m. In this last case 7 different possible hydrogen positions were tested by the refinements. Although the model with the highest disorder(H site 192l) gives the best goodness-of-fit parameters, the extra parameters and the unrealistically long N-H bond(0.11 nm) appear to rule it out. Two alternative models, with hydrogen at the 48h and 96j sites, respectively, give similar goodness-of-fit parameters and N-H bond lengths. Inasmuch as the 48h site model contains one fewer position parameter for the hydrogen atoms, it is suggested as the most likely structure for the compound at room temperature and yields an N-H bond length of 0.093 1 (15) nm. This result appears to be more realistic than the values, 0.08 ~ 0.082nm, reported by Ohoyama et al[19]. and by Noritake[20]on the same compound.

3.2 LiNH$_2$

Comparison of the neutron diffraction data for LiNH$_2$ (Fig. 2) with that for Li$_2$NH (Figs. 1a ~ c) immediately shows the additional complexity of the structure and the higher background due to the higher atomic hydrogen concentration. Nevertheless, the data refine easily and provide detailed information about the location of the hydrogen atoms. This structure is tetragonal(space group I − 4) and prior studies proposed two different models for the location of the Li atoms. Our results clearly distinguish between these two mod-
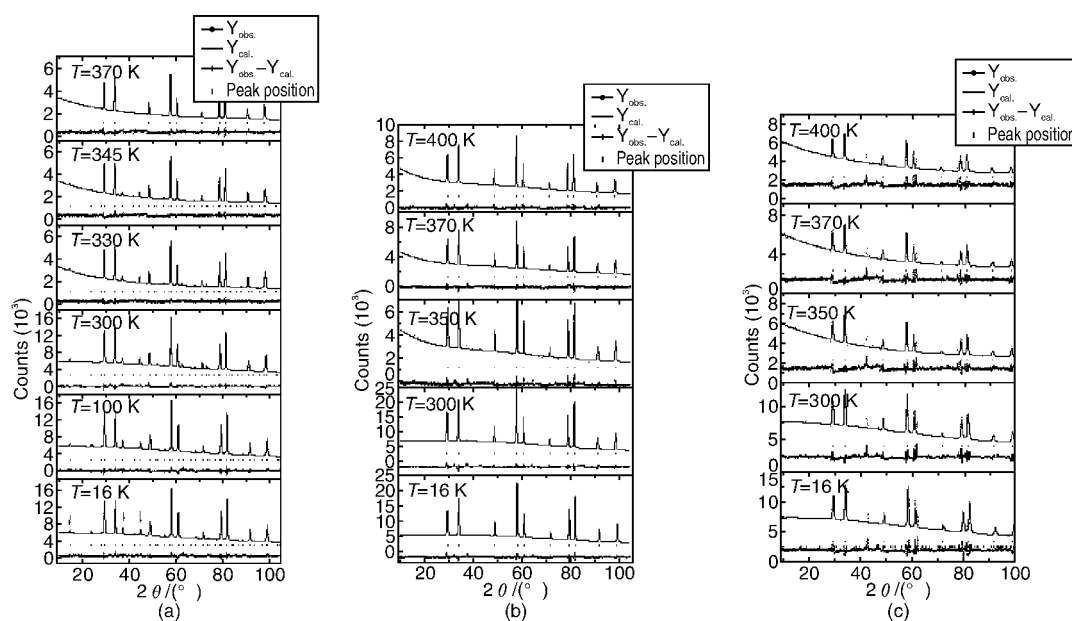
Fig 1   Refinement neutron diffraction patterns of α-Li$_2$NH(a), β-Li$_2$NH(b) and γ-Li$_2$NH(c) at different temperatures. The peaks marked with arrows in Fig. 1(a) indicate a low temperature phase

els, placing the Li atoms in three distinct positions, and generating two unique hydrogen sites. The N-H bond lengths are found to be 0.094 nm and 0.099 nm, much longer(and more realistic) than the values previously reported(0.071 ~ 0.076 nm). An in-situ neutron diffraction study of the decomposition of LiNH$_2$ under He and N$_2$ atmospheres was performed. Melting of LiNH$_2$ was observed under a N$_2$ atmosphere at 400 ℃, while decomposition to Li$_2$NH was observed in a He atmosphere, see Fig. 3. The source of these differences is not understood.
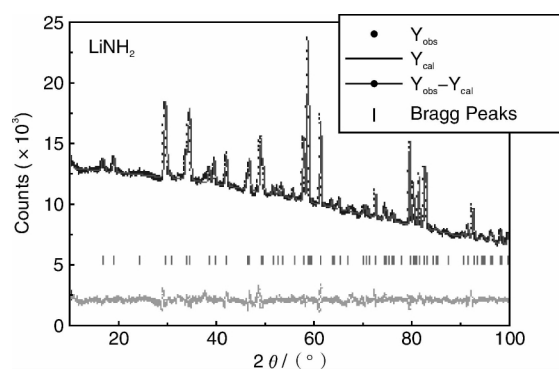

Fig 2   Neutron diffraction pattern of LiNH$_2$ at RT

3.3 Li$_4$BN$_3$H$_{10}$

Mixtures of LiNH$_2$-LiBH$_4$ in ratios of 3:1, 2:1 and 1:1 were prepared by ball milling of the precursors. The results of the milling appear to be nearly single phase materials with
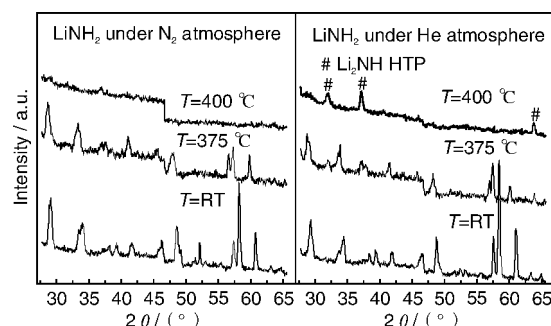

Fig 3   The temperature dependent ND patterns of LiNH$_2$ in N$_2$ and He atmospheres

stoichiometry Li$_4$N$_3$BH$_{10}$, Li$_3$N$_2$BH$_8$ and Li$_2$NBH$_6$, respectively. In each case a small impurity phase was observed and characterized. Filinchuk et al[21]. reported a new compound formed by reacting LiNH$_2$ and LiBH$_4$ in a ratio of 2 ~ 3:1. Although they report structural data based on single crystal x-ray diffraction, the N-H bonds they reported were unusually short and probably not reliable due to the use of x-rays; probing the valence electron density and not the proton positions. They report an ideal stoichiometry at the 3:1 ratio, although the sample they measured deviates from that value. Results on the same system by other investigators(Noritake et al[22] and Chater et al[23].) left unresolved inconsistencies. Thus, we synthesized several samples over this composition range for neutron diffraction analysis. Data at the 3:1 composition are shown in Fig. 4 before and after the ball milled

material was annealed to improve the crystallinity. It can be seen that the annealed sample diffracts well, even at the highest angles, giving highly precise refinement results. The analysis shows that the $LiBH_4$ group appears in the crystal structure as well-defined units, only weakly bonded to the $LiNH_2$ groups, which are cross-linked in the structure, see Fig. 5. This contrasts with the earlier results that show greater interactions between the two molecular species. We believe this is a consequence of the non-ideal stoichiometry of the earlier samples, leading to a mixing of the excess $LiBH_4$ on the $LiNH_2$ sites and an averaging of the difference in bonding between the different groups.
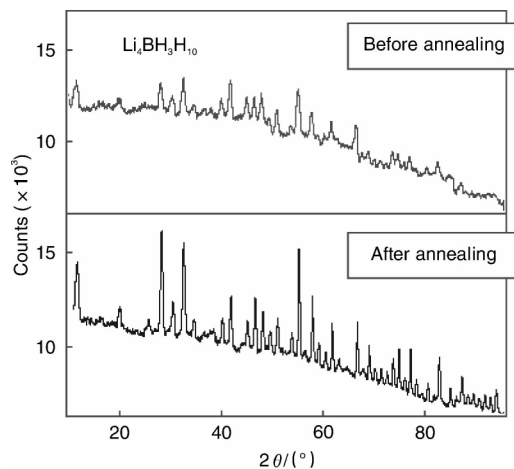

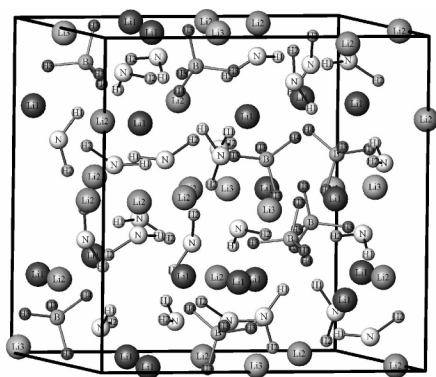Fig. 4   The ND patterns of $Li_4BN_3H_{10}$ before and after annealing at 190 ℃, measured at RT

Fig. 5   Crystal structure of $Li_4BN_3H_{10}$

In fact, our data on the 2:1 ratio sample show Bragg intensity ratios similar to the earlier neutron diffraction results, and can be refined on the "ideal" model. Modeling the disorder induced by the non-stoichiometry has proven to be quite difficult. These observations lead us to conclude that our results represent the ideal bonding between the imide and boro-

hydride groups. The N-H bonds in this material are found to be 0.104 nm and 0.110 nm, much longer than reported by Filinchuk (0.083 ~ 0.086 nm). Although our values are slightly longer than expected, we note an inverse correlation between the N-H bond lengths and the decomposition temperatures for these three systems.

3.4 NH_3BH_3, ND_3BH_3, NH_3BD_3 and ND_3BD_3

NH_3BH_3 was synthesized by the reaction of $(NH_4)_2CO_3$, and $NaBH_4$ in dry THF. NH_3BD_3 was prepared by the analogous reaction of $(NH_4)_2CO_3$, and $NaBD_4$ in dry THF. ND_3BH_3 was prepared by dissolving BH_3NH_3 in D_2O and stripping off the D_2O under vacuum. ND_3BD_3 was prepared by the analogous reaction; BD_3NH_3 in D_2O and purified by a similar procedure. All these samples are available for structural studies using neutron diffraction, including kinetic studies with in-situ neutron diffraction and several spectra have been collected. The neutron diffraction data were collected for ND_3BD_3 at different temperatures (Fig. 6). A phase transition has been observed. The resolution of the data is very good which allows us to accurately determine the structures of these materials and pursue further kinetic and thermodynamic studies.
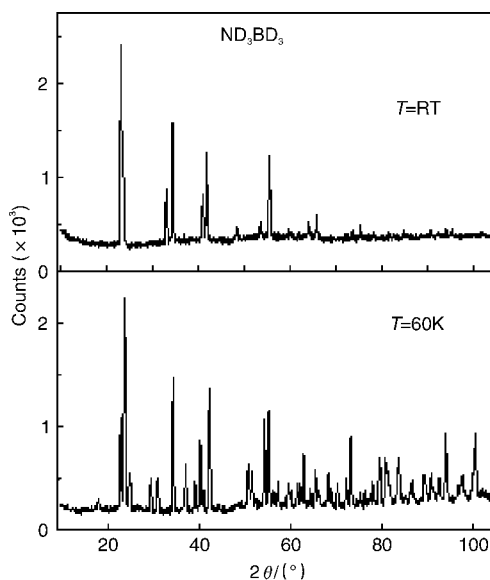

Fig 6   Neutron diffraction patterns of ND_3BD_3 at RT and 60K

Fig. 7 shows the typical neutron powder diffraction patterns of BH_3ND_3 collected from 16 K to 300 K. It is obvious that the diffraction pattern at 16 K shows more peaks and complexity as compared to the pattern at RT for all samples. Some peaks are merged and disappear as the temperature in-
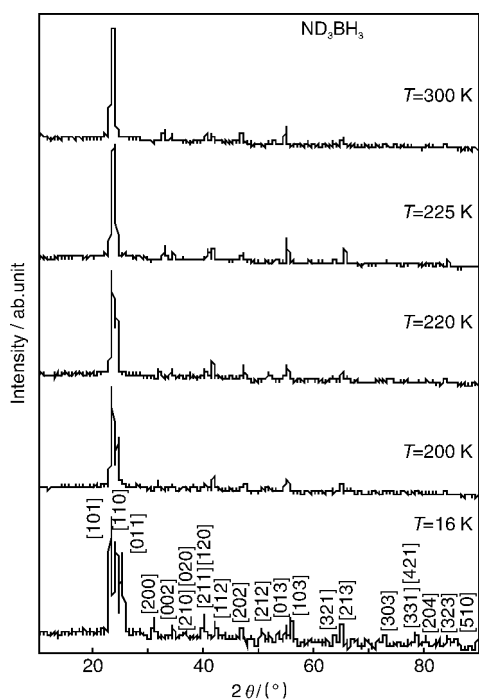
Fig. 7   Neutron powder diffraction patterns of BH_3ND_3 collected at different temperatures

creases. For example, peaks [011] and [110] shift to a low 2θ angle with increasing temperature, and finally merge with the peak [101], which indicating a rotation of the BH_3 and ND_3 groups along the c axis. At about 225 K, some new peaks appear and the number of the peaks is greatly reduced indicating a phase transition of much higher symmetry has occurred. It is found that at 16 K, the BH_3-ND_3 unit stacks along the c-axis with tilt angles between the N-B bond and the c axis and between the N-B bond and the b axis, respectively. The B-N bond is almost perpendicular to the a axis. As the temperature is increased, the BH_3-ND_3 groups start to reorient along the c axis, and the hydrogen atoms become disordered leading to the tetragonal phase transition around 225 K. As the temperature further increases, the unit cell volume and the bond length increase. At about 370 K, all the peaks disappear due to the melting of the samples, and decomposition occurs at the same time. The patterns above 225 K can be indexed as a body-centered tetragonal unit cell with space group I/4mm. As expected, all three compounds show the same phase transition. The refined lattice parameters of BH_3ND_3 at 16 K, are $a = 0.554\ 783(103)$ nm, $b = 0.467\ 632(86)$ nm, and $c = 0.500\ 291(78)$ nm, respectively, which are close to those of BD_3ND_3 and NH_3BD_3. The bond length between the nearest nitrogen and deuterium

atoms are 0.099 nm and 0.103 nm, and the B-H bond lengths are 0.141 nm and 0.120 nm at 16 K. The best refinement with Rw = 1.6% was obtained for RT data using the model proposed by Bowden et al[23]. The bond lengths between the nearest nitrogen and deuterium atom are 0.115 nm, and the B-H bond lengths are 0.131 nm at RT. As expected these values are longer than the single crystal XRD study, where the N-H bond is found to be 0.085 nm[23].

Figure 8 shows the dependence of the lattice parameters on the temperature from 16 K to RT. It can be seen that the c cell parameter remains unchanged in the orthorhombic phase from 16 K to 223 K. The lattice parameter a decreases from 0.554 8 nm to 0.525 2 nm, while the length of the b axis increases from 0.467 6 to 0.517 9 nm from 16 to 223 K. The cell parameters a and b, and the unit cell volume have abrupt changes at the phase transition region.
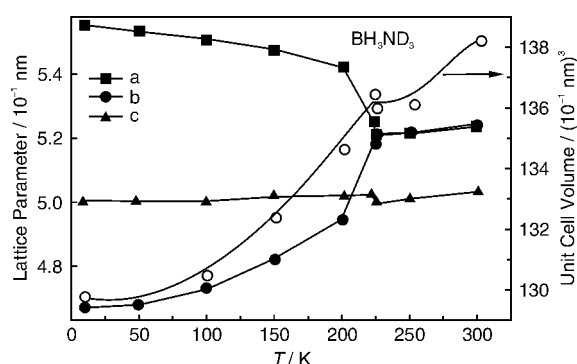

Fig. 8   The lattice parameters and unit cell volumes of BH_3ND_3 at different temperatures

4   Conclusions

Neutron diffraction is recognized for its potential importance to the study of hydrides because the scattering of neutrons by hydrogen or deuterium is proportionately stronger than for x-ray diffraction. We have shown that high quality data can be collected without deuteration for many systems of interest. The average N-H bond lengths are about 0.094, 0.096, 0.109 nm and 0.115 nm for Li_2NH, $LiNH_2$, $Li_4BN_3H_{10}$, and NH_3BH_3 respectively, which are substantially longer those the reported values, 0.076, 0.080, 0.085 nm. and 0.085 nm. The order of the decomposition temperatures $T_d(Li_2NH) > T_d(LiNH_2) > T_d(Li_4BN_3H_{10}) > T_d(NH_3BH_3)$ is coincidence to that of the average bond strengths.

References

[1] Bogdanovic B and Schwickardi M. Ti-Doped Alkali Metal Aluminium Hydrides as Potential Novel Reversible Hydrogen Storage Materials[J]. *Journal of Alloys and Compounds*, 1997, 253 – 254: 1 – 9.

[2] Graham D D, Culnane L F, Sulic M, *et al*. Ti EELS Standards for Identification of Catalytic Species in NaAlH$_4$ Hydrogen Storage Materials[J]. *Journal of Alloys and Compounds*, 2007, 446 – 447: 255 – 259.

[3] Wang J, Ebner A D, Ritter J A. Kinetic Behavior of Ti-Doped NaAlH$_4$ when Cocatalyzed with Carbon Nanostructures[J], *J Phys Chem B*, 2006, 110(35): 17 353 – 17 358.

[4] Brinks H W, Sulic M, Jensen C M, *et al*. TiCl$_3$-Enhanced NaAlH$_4$: Impact of Excess Al and Development of the Al$_{1-y}$Ti$_y$ Phase during Cycling[J]. *J Phys Chem B*, 2006, 110 (6): 2 740 – 2 745.

[5] Yoshino M, Komiya K, Takahashi Y, *et al*. Nature of the Chemical Bond in Complex Hydrides, NaAlH$_4$, LiAlH$_4$, LiBH$_4$ and LiNH$_2$[J]. *Journal of Alloys and Compounds*, 2005, 404 – 406: 185 – 190.

[6] Lodziana Z, Vegge T. Structural Stability of Complex Hydrides: LiBH$_4$ Revisited[J]. *Phys Rev Lett*, 2004, 93: 145 501 – 4.

[7] Züttel A, Wenger P, Rentsch S, *et al*. A High-Performance Hydrogen Generation System: Transition Metal-Catalyzed Dissociation and Hydrolysis of Ammonia-Borane [J]. *Journal of Power Sources*, 2003, 156(2): 190 – 194

[8] Vajo J J, Skeith S L, Mertens F. Reversible Storage of Hydrogen in Destabilized LiBH$_4$[J]. *J Phys Chem B*, 2005, 109: 3 719 – 3 722.

[9] Hess N J, Schenter G K, Hartman M R, *et al*. Neutron Powder Diffraction and Molecular Simulation Study of the Structural Evolution of Ammonia Borane from 15 to 340 K[J]. *J Phys Chem A*, 2009, 113(9): 5 723 – 5 735.

[10] Chandra M, Xu Q. A High-Performance Hydrogen Generation System: Transition Metal-Catalyzed Dissociation and Hydrolysis of Ammonia-Borane [J]. *J Power Sources*, 2006, 156 (2): 190 – 194.

[11] Gutowska A, Li L, Shin Y, *et al*. Nano-Scaffold Mediates Hydrogen Release and Reactivity of Ammonia Borane[J]. *Angewandte Chemie International Edition*, 2005, 44(23): 3 578 – 3 582.

[12] Pinkerton F E, Meyer M S, Meisner G P, *et al*. Phase Boundaries and Reversibility of LiBH$_4$/MgH$_2$ Hydrogen Storage Material [J]. *J Phys Chem C*, 2007, 111(35): 12 881 – 12 885.

[13] Vajo J J, Olson G L. Hydrogen Storage in Destabilized Chemical Systems[J]. *Scripta Materialia*, 2007, 56(10): 829 – 834.

[14] Li H W. Orimo S, Nakamori Y, *et al*. Materials Designing of Metal Borohydrides: Viewpoints from Thermodynamical Stabilities[J]. *Journal of Alloys and Compounds*, 2007, 446 – 447: 315 – 318

[15] Matsunaga T, Buchte F R, Miwa K, *et al*. Magnesium Borohydride: A new Hydrogen Storage Material[J]. *Renewable Energy* 2008, 33(2): 193 – 196.

[16] Yang J B, Cai Q, Zhou X D, *et al*. Crystal and Electronic Structures of the Complex Hydride Li$_4$BN$_3$H$_{10}$[J]. *J Appl Phys*, 2007, 102: 033 507 – 033 511.

[17] Chen P, Xiong Z, Luo J, *et al*. Interaction of Hydrogen with Metal Nitrides and Imides[J]. *Nature*, 2002, 420: 302 – 304.

[18] Hu Y H, Ruckenstein E. High Reversible-Hydrogen Storage Capacity with Ultra-Fast Kinetics of LiNH$_2$/Li$_3$N[J]. *Ind Eng Chem Res*, 1005, 44: 1 510 – 1 513.

[19] Ohoyama K, Nakamori Y, OrimoS, *et al*. Revised Crystal Structure Model of Li$_2$NH by Neutron Powder Diffraction[J]. *J Phys Soc Jpn*, 2005, 74: 483 – 487.

[20] Noritake T, Nozaki H, Aoki M, *et al*. Crystal Structure and Charge Density Analysis of Li$_2$NH by Synchrotron X-ray Diffraction[J]. *Journal of Alloys and Compounds*, 2005, 393 (1 – 2): 264 – 268.

[21] Filinchuk Y E, Yvon K, Meisner G P, *et al*. On the Composition and Crystal Structure of the New Quaternary Hydride Phase Li$_4$BN$_3$H$_{10}$[J]. *Inorg Chem*, 2005, 45: 1 433 – 1 435.

[22] Noritake T, Aoki M, Towata S, *et al*. Crystal Structure Analysis of Novel Complex Hydrides Formed by the Combination of LiBH$_4$ and LiNH$_2$[J]. *Appl Phys*, 2006, A83: 277 – 279.

[23] Chater P A, David W I F, Johnson S R, *et al*. Synthesis and Crystal Structure of Li$_4$BH$_4$(NH$_2$)$_3$ [J]. *Chem Commun*, 2006, 23: 2 439 – 2 441.

[24] Bowden Mark E, Gainsford Graeme J, Robinson Ward T. Room-Temperature Structure of Ammonia Borane[J]. *Australian J Chem*, 2007, 60(3): 149 – 153.